

NATIONAL ADVISORY COMMITTEE FOR AERONAUTICS

TECHNICAL NOTE 3647

INVESTIGATION OF THE COMPRESSIVE STRENGTH AND CREEP
LIFETIME OF 2024-T ALUMINUM-ALLOY SKIN-STRINGER
PANELS AT ELEVATED TEMPERATURES

By Eldon E. Mathauser and William D. Deveikis

Langley Aeronautical Laboratory
Langley Field, Va.



Washington
May 1956



NATIONAL ADVISORY COMMITTEE FOR AERONAUTICS

TECHNICAL NOTE 3647

INVESTIGATION OF THE COMPRESSIVE STRENGTH AND CREEP
LIFETIME OF 2024-T ALUMINUM-ALLOY SKIN-STRINGER
PANELS AT ELEVATED TEMPERATURES

By Eldon E. Mathauser and William D. Deveikis

SUMMARY

The experimental results of an investigation to determine compressive strength and creep lifetime of 2024-T aluminum-alloy skin-stringer panels at room temperature and 400° F are presented. The results of strength tests at room temperature and 400° F are compared with predicted strength obtained from methods given in the literature for estimating crippling strength of short panels and for predicting column strength of longer panels. Creep lifetime curves are presented for four values of slenderness ratio and creep characteristics of the panels are discussed. A method which makes use of time-dependent compressive stress-strain (isochronous) curves for predicting creep lifetime of panels is presented.

INTRODUCTION

Since aircraft structures will be subjected to elevated temperatures during high-speed flight, a knowledge of the elevated-temperature strength and creep lifetime of structural components is becoming increasingly important. Studies have been made recently by the National Advisory Committee for Aeronautics to obtain some experimental data on elevated-temperature strength and creep behavior of columns, plates, and multiweb box beams (refs. 1 to 3). The experimental results from skin-stringer panels reported in the present paper are a continuation of the previous program concerned with elevated-temperature strength and creep behavior of structural components. Some observations obtained in this study of skin-stringer panels were presented in reference 4.

In the present study, 38 skin-stringer panels of identical cross section and 4 different lengths were tested. Compressive strength tests were made at room temperature and 400° F on 16 panels. Creep tests were performed at 400° F on the remaining panels. All panels were made of 2024-T3 aluminum-alloy sheet and 2024-T4 aluminum-alloy Z-section extrusions.

The experimental results of the strength tests at room temperature and 400° F are compared with predicted strength obtained from methods given in the literature for estimating crippling strengths of short panels (ref. 5) and for predicting column strength of long panels (ref. 6). Lifetime curves obtained in the creep tests at 400° F are presented and creep behavior of the skin-stringer panels is discussed. The use of time-dependent material compressive stress-strain (isochronous) curves for predicting creep lifetime of panels is investigated.

SYMBOLS

A, B, K	creep constants
b	width, in.
c	end-fixity coefficient in Euler column formula
E_s	secant modulus, ksi
\bar{E}_t	tangent modulus of curve showing average stress against unit shortening from a short panel, ksi
L	length of panel, in.
r	constant or minimum rate of unit shortening obtained in creep test of panel (corresponds to constant or secondary creep rate in material creep test), in./in./hr
t	thickness, in.
T	temperature, $^{\circ}$ F
ϵ	strain
$\bar{\epsilon}$	unit shortening
$\bar{\epsilon}_f$	unit shortening at maximum load
σ	stress, ksi
σ_{cy}	0.2-percent-offset compressive yield stress, ksi
$\bar{\sigma}$	average stress, ksi
$\bar{\sigma}_b$	average stress for panel at which column bending begins (corresponds to tangent-modulus stress for columns), ksi

$\bar{\sigma}_f$	average stress at maximum or failing load, ksi
ρ	radius of gyration, in.
τ	time, hr
τ_{cr}	failure time, hr

TEST SPECIMENS, EQUIPMENT, AND PROCEDURES

The cross section of the skin-stringer panels tested in the present investigation is shown in figure 1. The width-thickness ratio for the skin in each bay was 50 and for the webs in the stringers, 12.5. Four different panel lengths with corresponding nominal slenderness ratio values of 18, 36, 64, and 92 were tested. For the skin, 2024-T3 aluminum-alloy sheet was used and for the stiffeners, 2024-T4 aluminum-alloy Z-section extrusions. The ends of the specimens were ground flat and parallel to obtain uniform bearing on the ends. All specimens were tested flat-ended without side support.

All panels were tested at room and elevated temperature with the test equipment shown in figure 2. The hydraulic testing machine was used to apply load for determining maximum compressive strength and the dead-weight apparatus was used to apply constant load for determining creep behavior. The panels were mounted between heated rams shown in figure 3. In this view the furnace has been removed. Shortening of the panels was determined during the tests from measurements of the relative motion between the ends of the specimens. This motion was transferred to two linear variable differential transformers by means of rods extending from the upper and lower rams. Shortening was recorded autographically against load in the compressive strength tests and in the creep tests, against time. Spring clips were used to support iron-constantan thermocouples on the panel skin during the tests at 400° F. The temperature of the specimen was maintained within $\pm 5^{\circ}$ F of the test temperature.

All panel specimens were alined in the rams before heating began. Approximately 1/2 hour was required to heat the specimen to the 400° F test temperature. Before load was applied, the panels were exposed to test temperature for periods which are noted in the sections on test results. Load was applied in the compressive strength tests at a rate that produced average unit shortening of 0.002 per minute. In the creep tests, the dead load was applied in approximately 1 minute and was maintained on the specimen until the panel collapsed or up to a maximum of 6 to 7 hours. If the panel did not collapse within this period, the test

was discontinued. Failure time in the creep tests, ranging from several minutes to a few hours, was measured from the time total load was applied until collapse occurred.

RESULTS AND DISCUSSION

Compressive Strength Tests

Experimental data.— Compressive behavior of the panels determined from the strength tests is shown in figure 4. Average stress is plotted against unit shortening for one panel of each slenderness ratio tested at room temperature and at 400° F after exposure at 400° F for various times. Compressive stress-strain curves for the 2024-T3 aluminum-alloy sheet obtained at the same test temperatures with similar exposure times are also shown and are labeled as $\sigma - \epsilon$. Facilities were not available for obtaining elevated-temperature compressive stress-strain properties of the stringers; however, it is assumed that the data given in figure 4 for the 2024-T3 aluminum-alloy sheet satisfactorily approximate the compressive stress-strain properties of the 2024-T4 aluminum-alloy stringers.

Material and panel compressive properties obtained in tests at room temperature for different exposure times are shown in figures 4(a) and 4(b). The material compressive yield stress was considerably increased by exposing the material at 400° F for 10 hours prior to testing at room temperature. For the panels exposed at 400° F for 10 hours and tested at room temperature, a substantial increase in strength was also obtained. This increased strength can be expected with 2024-T aluminum alloy and would not be obtained with most other structural materials.

In the 400° F tests, shown in figures 4(c) and 4(d), the material compressive yield stress was greater for the 10-hour exposure time than for the 1/2-hour exposure time. In addition, a marked difference was obtained in the shape of the material stress-strain curves. The strengths of the panels tested at 400° F also showed some effects of the two different exposure times. The strengths of all panels exposed at 400° F for 10 hours prior to testing was greater than the strengths of the panels exposed at 400° F for 1/2 hour before testing except for the longest panel $\left(\frac{L}{\rho} = 92\right)$.

No significant change was obtained in the unit shortening at maximum load for all panels as a result of the different exposure times; that is, the maximum strengths were obtained at approximately constant values of unit shortening for each panel length. A summary of the significant experimental data obtained in the compressive strength tests is given in table I.

Prediction of maximum strength of short panels. - For the short panels ($\frac{L}{\rho} = 18$), the maximum or crippling strength was obtained by summing the predicted strength of the sheet and stringer plate elements. The maximum strengths of the plate elements were determined from the relation

$$\bar{\sigma}_f = 1.60 \sqrt{E_s \sigma_{cy} \frac{t}{b}} \quad (1)$$

given in reference 5. (The secant modulus E_s is evaluated from the material compressive stress-strain curve at $\bar{\sigma}_f$.) The maximum stresses calculated for each plate element from equation (1) were weighed according to areas to obtain the average stress at maximum load for the short panels as follows:

$$\bar{\sigma}_f = \frac{\sum \bar{\sigma}_f A_S + \sum \bar{\sigma}_f A_Z}{\sum A_S + \sum A_Z} \quad (2)$$

where A_S and A_Z refer to the cross-sectional areas of the skin and Z-section stringer, respectively. The maximum strength of the stringer was obtained by calculating $\bar{\sigma}_f$ for the web from equation (1) and assuming that the flanges of the stringer would fail at the maximum stress determined for the web.

The calculated strengths of the short panels ($\frac{L}{\rho} = 18$) are given in table I. The agreement between the predicted and experimental strengths is satisfactory.

Prediction of column strength of long panels. - Column strength of the longer panels ($L/\rho > 18$) was determined by the method suggested in reference 6. This method makes use of the experimental average stress against unit shortening curve from the shortest panel ($\frac{L}{\rho} = 18$) as an effective stress-strain curve from which values of \bar{E}_t are obtained. These values are then substituted into the generalized Euler column formula

$$\bar{\sigma}_b = \frac{c\pi^2 \bar{E}_t}{\left(\frac{L}{\rho}\right)^2} \quad (3)$$

to determine strength of longer panels of identical cross section. In the present investigation, the curves of average stress against unit

shortening shown in figure 4 for $\frac{L}{p} = 18$ were used to predict column strength of the long panels. The results, obtained with an end-fixity coefficient of 3.75 (see ref. 7), are given in table I and are compared with experimental results in figure 5. Crippling stresses calculated for $\frac{L}{p} = 18$ by the method described in the preceding section as well as the Euler buckling stresses are also shown in figure 5.

The predicted strengths of the long panels shown in the upper plot of figure 5 are in good agreement with the experimental results. In the lower plot of figure 5, the predicted strengths are unconservative compared with the experimental strengths of the long panels. This result may be due in part to the use of the curve of average stress against unit shortening for $\frac{L}{p} = 18$ for predicting strength of the longer panels.

The length of these short panels was relatively small compared with the stringer spacing. End effects which are associated with short-length specimens may have influenced the shape of the curve for experimental average stress against unit shortening.

Prediction of average stress against unit shortening curves. - Inasmuch as the curve of average stress against unit shortening for a short panel appears to be useful for predicting the column strength of longer panels, a study was made to determine whether the method given in reference 6 would successfully predict such curves in the present investigation. In reference 6 a procedure is described for obtaining the curve of average stress against unit shortening for a short panel of one material when a curve for experimental average stress against unit shortening obtained from a panel of identical geometry and different material is available. Compressive stress-strain curves for both materials are also required.

Curves of average stress against unit shortening predicted in the present investigation for $\frac{L}{p} = 18$ at 400° F for two different exposure times are shown in figure 6. The predicted curve shown in figure 6(a) was obtained by using the method outlined in reference 6 and material stress-strain data in figure 4(a) and figure 4(c) and the curve for average stress against unit shortening for $\frac{L}{p} = 18$ in figure 4(a). The ordinates of the predicted curve were adjusted as described in reference 6 so that the maximum ordinate would agree with the predicted crippling strength given in table I. Close agreement between the predicted and experimental curves was obtained. Column strengths of longer panels obtained from the predicted curve would agree with strengths predicted from the experimental curve.

The predicted curve shown in figure 6(b) was obtained with the aid of material stress-strain data given in figure 4(b) and figure 4(d) and the average stress against unit shortening curve for $\frac{L}{\rho} = 18$ given in figure 4(b). Although the agreement between the two curves in figure 6(b) is not so satisfactory as that obtained in figure 6(a), the largest difference between stresses at any value of unit shortening is about 5 percent. Column strengths of panels with L/ρ less than 50 determined from the predicted curve would range up to 5 percent less than strengths determined from the experimental curve. For panels with L/ρ greater than 50, column strengths obtained from either curve of figure 6(b) are identical.

Creep Tests

Experimental panel creep curves.—Creep curves which are representative of the data obtained from tests at 400° F for each slenderness ratio are shown in figure 7. The panel designation, the applied compressive stress, and the ratio of applied stress to the maximum stress obtained in the compressive strength tests for each slenderness ratio are given. All panels had been exposed at 400° F for 10 hours prior to loading. This exposure produced relatively stable material properties which would not be altered appreciably by additional exposure for short periods at the same temperature. Inasmuch as the creep tests were of short duration, the observed behavior of the panels in the creep tests is assumed to reflect structural behavior independent of significant changes in material properties. Buckles were produced in the skin of all panels immediately upon loading. The buckles increased in depth during the creep tests and were accompanied by lateral deflection of the stiffeners until collapse occurred. A summary of the creep test results is given in table II.

The results from the creep tests indicate that small changes in applied stress produce large changes in panel lifetime. For example, for panels 27 and 28 ($\frac{L}{\rho} = 36$), a stress decrease of approximately 3 percent increased the panel lifetime by a factor of 5.

Panel lifetime curves.—Lifetime curves obtained from the creep tests of panels which failed within the test period are shown in figure 8. Straight lines have been drawn through the data for each value of slenderness ratio. The solid symbols on the vertical axis indicate the average stress at maximum load obtained in the compressive strength tests of panels tested at 400° F after 10 hours of exposure at 400° F.

The results from the panel creep tests (fig. 8) show more scatter than results from creep tests of plates (fig. 11 of ref. 2). This result is expected because initial out-of-straightness of the stringers, comparable with out-of-straightness of columns, may have a significant effect

on panel lifetime. In plates, however, the effects of initial imperfections may be insignificant compared with the buckles that are produced either by loading or by gradual growth during the creep tests.

Creep behavior of panels. - The creep curves given in figure 7 indicate that most panels exhibited a constant or minimum rate of unit shortening for a large part of the panel lifetime. The minimum rates of unit shortening obtained from the creep curves for all panels tested are plotted in figure 9. Minimum creep rates for 2024-T3 aluminum-alloy sheet tested in tension (from ref. 8) are also included in figure 9. All panels tested showed higher rates of unit shortening at all stresses than were obtained in the tensile creep tests of the material.

An indication of the magnitude of the unit shortening that existed in the panels prior to failure in the creep tests is given in figure 10. In this figure, the creep lifetime curves are reproduced from figure 8 for each slenderness ratio. In addition, curves are shown which indicate the stress-time combinations that produce 0.2-percent permanent shortening in the panels. Data required for plotting these curves were obtained from the creep curves of all panels tested, examples of which are shown in figure 7. The long panels ($\frac{L}{p} = 64$ and $\frac{L}{p} = 92$) failed at approximately 0.2-percent permanent shortening. For the shorter panels ($\frac{L}{p} = 18$ and $\frac{L}{p} = 36$), 0.2-percent permanent shortening was obtained in many cases before 50 percent of the panel lifetime was exhausted.

A summary of the creep behavior of all panels is shown in figure 11. The curves which show average stress plotted against unit shortening for each slenderness ratio are reproduced from figure 4(d). The key shown at the top of figure 11 shows a typical panel creep curve and indicates various creep stages. The termination of each creep stage is indicated by a symbol. These symbols are shown on the plots for each slenderness ratio to indicate the magnitude of unit shortening obtained at the end of each creep stage in the panel creep tests. The horizontal dot-dashed line shown on the plot for $\frac{L}{p} = 18$ indicates the magnitude of the stress applied on panel 17 in the creep test. Unit shortening obtained immediately upon loading is indicated by the intersection of this horizontal line with the curve for average stress against unit shortening. The panel then began to shorten at a decreasing rate throughout the primary creep region until unit shortening indicated by the circular symbol was obtained. Additional unit shortening occurred at a constant rate in the secondary creep region up to the point indicated by the square symbol. (Note that the unit shortening obtained at the termination of the secondary creep rate corresponds closely to ϵ_f , the unit shortening obtained at maximum load in the strength tests.) Unit shortening beyond the value indicated by the

square symbol occurred at an accelerated rate in the tertiary creep region until the panel collapsed. The magnitude of the unit shortening at collapse is indicated by the diamond symbol. Primary and tertiary creep occurred during a relatively small percentage of the panel lifetime. Constant rate of unit shortening was obtained in most cases for approximately 75 percent of the panel lifetime. Collapse usually occurred soon after accelerated unit shortening began.

Determination of time-dependent stress-strain (isochronous) curves. - In the present investigation, a study was made to determine whether material compressive creep curves in the form of time-dependent stress-strain (isochronous) curves could be used to predict panel lifetime. Time-dependent stress-strain curves have previously been used for determining creep lifetime of plates (ref. 2). In order to establish time-dependent stress-strain curves in the present investigation, compressive creep curves for the 2024-T3 aluminum-alloy sheet at 400° F were obtained from tests of plate specimens ($\frac{b}{t} = 20$) tested in V-groove fixtures. The plate material was heat treated at 400° F for 10 hours prior to testing. Test procedures described in reference 2 were used for these plate tests. The experimental results obtained from the plate tests are given in figure 12. The primary and secondary creep stages for the creep curves of this figure were expressed in the following form:

$$\epsilon = \frac{\sigma}{E_s} + Ae^{B\sigma\tau^K} \quad (4)$$

The values of A, B, and K which produce the best agreement with the curves of figure 12 (σ in ksi, τ in hours) are:

$$A = 2.00 \times 10^{-5}$$

$$B = 0.120$$

$$K = 0.200$$

The secant modulus E_s was determined from the material compressive stress-strain curve given in figure 4(d). Strains calculated from equation (4) for different stresses and for times of 0.1, 1, and 10 hours are plotted as time-dependent stress-strain (isochronous) curves in figure 13. It is assumed that the curves of figure 13 describe the creep behavior of the material in both the panel skin and the stiffeners. The dashed curve given in figure 13 is the material compressive stress-strain curve for 10 hours exposure at 400° F.

Creep failure stresses for short panels. - The stresses that produce creep failure of the short panels ($\frac{L}{p} = 18$) in a given time were determined by using a method analogous to that previously described in the section entitled "Prediction of maximum strength of short panels." Values of time-dependent secant modulus $E_s(\tau)$ and time-dependent compressive yield stress $\sigma_{cy}(\tau)$ obtained from figure 13 were substituted into equation (1) to determine the stresses that produce creep failure of the plate elements of the panel. The average stress that produces creep failure of the panel skin $\bar{\sigma}_s(\tau)$ and the average stress that produces creep failure of the plate elements of the Z-section stiffener in the same time $\bar{\sigma}_Z(\tau)$ were weighed according to areas of these elements, as shown in equation (2), to obtain the average stress that will fail the stiffened panel in a given time.

The calculated average stresses which will fail the panel in 0.1, 1, and 10 hours ranged from 6 percent less to 8 percent greater than the experimental results obtained from figure 8 for $\frac{L}{p} = 18$. Additional creep tests of panels of different cross sections will be needed to determine whether lifetimes can be estimated for such panels with comparable results.

Creep failure stresses for long panels. - In order to determine stresses which produce creep failure of the longer panels ($\frac{L}{p} > 18$), a study was made to establish whether curves of time-dependent average stress against unit shortening could be used in a manner analogous to the use of curves of experimental average stress against unit shortening for predicting column strength of long panels. (See section entitled "Prediction of column strength of long panels".) The method described in reference 6 was used to obtain the curves for time-dependent average stress against unit shortening $\bar{\sigma}(\tau)-\bar{\epsilon}(\tau)$ for short panels. The predicted $\bar{\sigma}(\tau)-\bar{\epsilon}(\tau)$ curves, shown in figure 14, were obtained with the aid of material stress-strain data given in figure 4(a) and the curve for average stress against unit shortening for $\frac{L}{p} = 18$ from figure 4(a) as well as the time-dependent stress-strain curves given in figure 13. The predicted curves of figure 14 indicate the magnitude of the unit shortening obtained for different stresses at 0.1, 1, and 10 hours for panels of $\frac{L}{p} = 18$. The maximum ordinates of these curves indicate stresses that will produce creep failure of the stiffened panels at 0.1, 1, and 10 hours and should be in agreement with the experimental results shown in figure 8 for $\frac{L}{p} = 18$. The maximum ordinates of the predicted curves differed from the experimental results in figure 8 by amounts ranging from 2 to 6 percent. Linear adjustments were made in the ordinates of the predicted curves by using procedures given in reference 6 to bring the maximum ordinates into

agreement with the experimental results of figure 8. The curves shown in figure 14 include these adjustments in ordinates.

Values of time-dependent tangent moduli $\bar{E}_t(\tau)$ were obtained from the curves of figure 14 for substitution into equation (3) to obtain creep lifetime of longer panels. Results obtained from such calculations are shown by the curves in figure 15. The symbols indicate values of stress obtained from the curves of figure 8 for each value of L/ρ at 0.1, 1, and 10 hours. Fair agreement is obtained between the predicted and experimental lifetime for the shorter panels. For the longer panels, the predicted results are conservative compared with the experimental results.

The use of material compressive creep data plotted as time-dependent stress-strain (isochronous) curves for determining stresses that produce creep failure of skin-stringer panels has been presented. For short panels, time-dependent stress-strain curves were used in conjunction with methods that are available for determining crippling strength. For longer panels, stresses that produce creep failure were determined by using both time-dependent stress-strain curves and a curve for experimental average stress against unit shortening from a short panel to obtain curves for time-dependent average stress against unit shortening. Additional experimental creep data for panels of other cross sections and different materials will be needed to determine whether these methods will be satisfactory for general application in predicting panel lifetime.

CONCLUDING REMARKS

The experimental results of an investigation to determine compressive strength and creep lifetime of 2024-T aluminum-alloy skin-stringer panels have been presented. The results of the strength tests at room temperature and 400° F compared satisfactorily with predicted strengths obtained from methods given in the literature for estimating crippling strength of short panels and for predicting column strength of longer panels. A method given in the literature for predicting average stress against unit shortening curves was satisfactory, in general, for obtaining these curves in the present investigation.

Creep lifetime curves were presented for the panels for four values of slenderness ratio and creep characteristics of the panels were discussed. Time-dependent material compressive stress-strain (isochronous) curves were used to obtain creep lifetime of short panels and curves of

time-dependent average stress against unit shortening were used to obtain creep lifetime of long panels.

Langley Aeronautical Laboratory,
National Advisory Committee for Aeronautics,
Langley Field, Va., January 30, 1956.

REFERENCES

1. Mathauser, Eldon E., and Brooks, William A., Jr.: An Investigation of the Creep Lifetime of 75S-T6 Aluminum-Alloy Columns. NACA TN 3204, 1954.
2. Mathauser, Eldon E., and Deveikis, William D.: Investigation of the Compressive Strength and Creep Lifetime of 2024-T3 Aluminum-Alloy Plates at Elevated Temperatures. NACA TN 3552, 1956. (Supersedes NACA RM L55E11b.)
3. Mathauser, Eldon E.: Investigation of Static Strength and Creep Behavior of an Aluminum-Alloy Multiweb Box Beam at Elevated Temperatures. NACA TN 3310, 1954.
4. Mathauser, Eldon E., and Libove, Charles: Preliminary Investigations of Strength Characteristics of Structural Elements at Elevated Temperatures. NACA RM L53E04a, 1953.
5. Anderson, Roger A., and Anderson, Melvin S.: Correlation of Crippling Strength of Plate Structures With Material Properties. NACA TN 3600, 1956.
6. Dow, Norris F., and Anderson, Roger A.: Prediction of Ultimate Strength of Skin-Stringer Panels From Load-Shortening Curves. Preprint No. 431, S.M.F. Fund Preprint, Inst. Aero. Sci., Jan. 1954.
7. Hickman, William A., and Dow, Norris F.: Data on the Compressive Strength of 75S-T6 Aluminum-Alloy Flat Panels With Longitudinal Extruded Z-Section Stiffeners. NACA TN 1829, 1949.
8. Dorn, J. E., and Tietz, T. E.: Creep and Stress-Rupture Investigations on Some Aluminum Alloy Sheet Metals. Preprint 26, A.S.T.M., 1949, pp. 1-17.

TABLE I.- COMPRESSIVE STRENGTH TEST RESULTS

Panel	L, in.	L/ρ	Test temperature, °F	Exposure time at 400° F prior to testing, hr	$\bar{\sigma}_f$, ksi	$\bar{\epsilon}_f$	Predicted $\bar{\sigma}_f$, ksi (a)
1	3.52	18.3	Room	None	33.0	0.00710	35.0
2	6.82	36.3	Room	None	30.4	.00505	31.9
3	12.00	64.6	Room	None	28.5	.00355	28.8
4	17.22	92.4	Room	None	25.2	.00255	25.2
5	3.50	18.3	400	1/2	30.1	.00625	29.9
6	6.92	36.3	400	1/2	28.8	.00570	29.1
7	12.00	64.6	400	1/2	25.3	.00360	26.3
8	17.22	92.4	400	1/2	23.2	.00265	22.0
9	3.41	18.3	Room	10	44.5	.00700	42.0
10	6.78	36.4	Room	10	41.8	.00585	43.7
11	11.94	64.1	Room	10	38.2	.00460	40.3
12	17.03	91.4	Room	10	29.0	.00305	32.9
13	3.38	18.1	400	10	34.2	.00615	32.9
14	6.78	36.4	400	10	32.6	.00550	33.7
15	11.93	64.0	400	10	27.6	.00370	31.3
16	17.04	91.5	400	10	21.8	.00280	27.1

^aCrippling strength of the short panels $\left(\frac{L}{\rho} = 18\right)$ determined from equation (2); column strength of the longer panels $\left(\frac{L}{\rho} > 18\right)$ determined from equation (3).

TABLE II.- CREEP TEST RESULTS AT 400° F

[All panels were exposed for 10 hours at 400° F
before application of load]

Panel	L, in.	L/ρ	σ, ksi	σ/σ _f	τ _{cr} , hr	r, in./in./hr
17	3.42	18.9	30.5	0.893	0.25	0.0118
18	3.42	18.7	30.1	.880	.20	.0151
19	3.42	18.8	28.9	.846	.68	.00424
20	3.42	18.7	28.4	.830	1.48	.00147
21	3.42	18.7	28.1	.822	1.20	.00209
22	3.42	18.3	27.3	.792	3.69	.000978
23	3.42	18.9	26.8	.784	^a 4.09	.000635
24	3.42	18.5	24.9	.728	^a 6.90	.000300
25	6.78	37.1	28.6	.878	.38	.00682
26	6.78	37.2	27.5	.844	.82	.00229
27	6.90	37.0	26.8	.822	1.24	.00219
28	6.78	36.3	26.0	.800	^a 6.02	.000446
29	6.90	37.0	24.4	.750	^a 6.40	.000335
30	6.78	37.1	23.4	.718	^a 6.50	.000149
31	12.10	64.9	26.5	.960	.79	.00155
32	12.07	64.7	25.4	.920	1.58	.000570
33	12.05	64.6	24.8	.899	3.14	.000208
34	11.97	64.2	24.6	.892	4.48	.000264
35	17.22	92.5	21.4	.982	2.85	.000105
36	17.22	92.5	21.2	.972	^a 6.52	.0000438
37	17.20	92.2	21.1	.968	^a 6.20	.0000450
38	17.03	91.4	20.8	.954	^a 6.80	.0000462

^aCreep test stopped at indicated time before failure occurred.

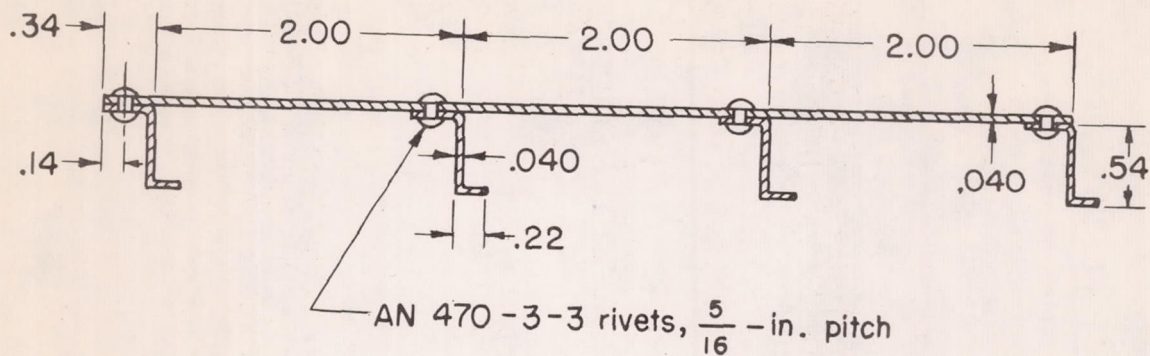


Figure 1.- Panel cross section.

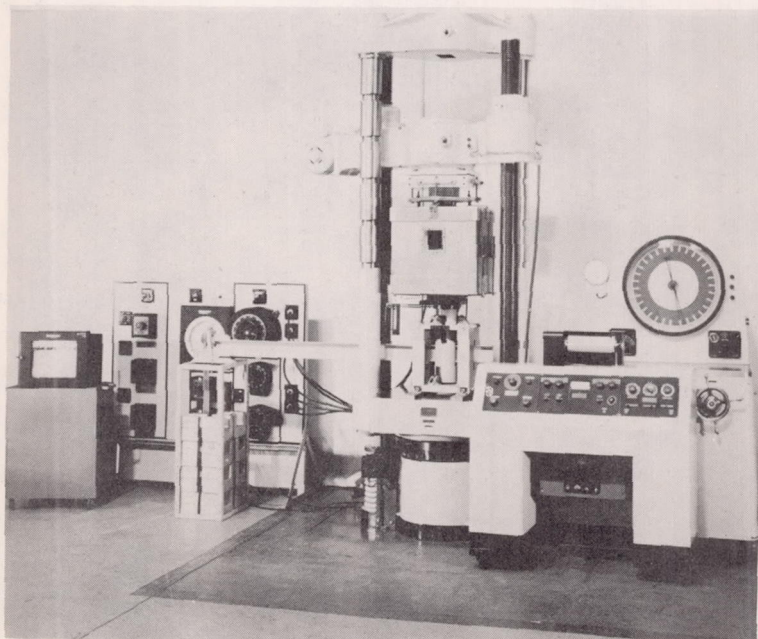


Figure 2.- Test equipment.

L-78962

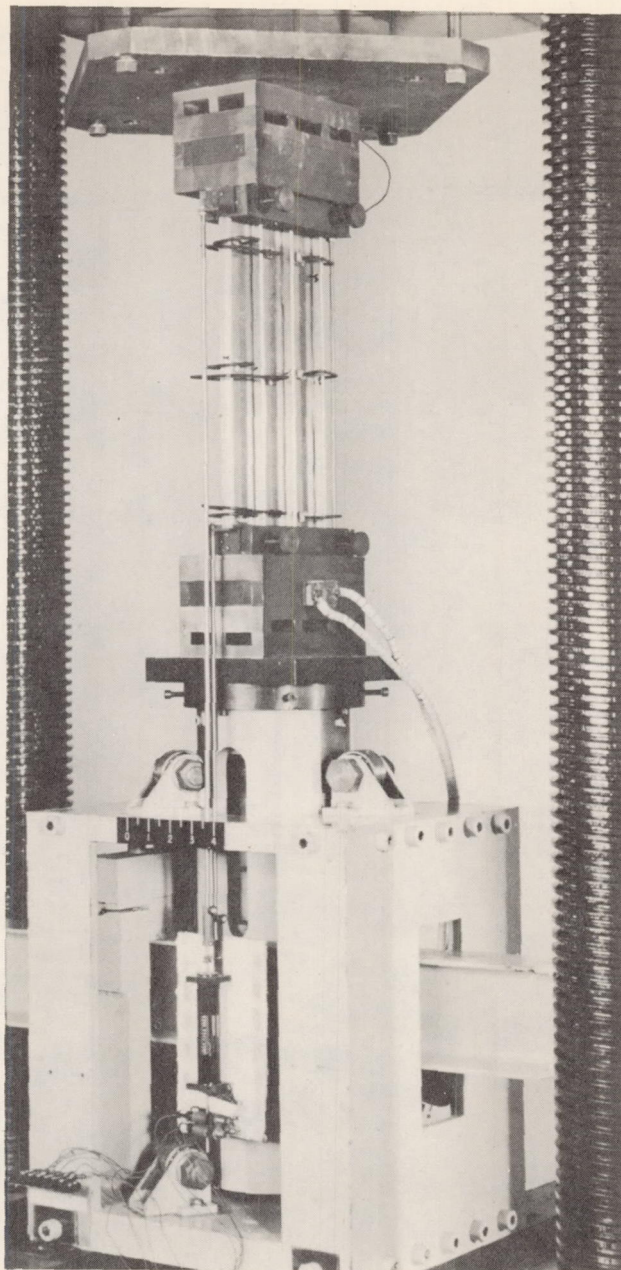
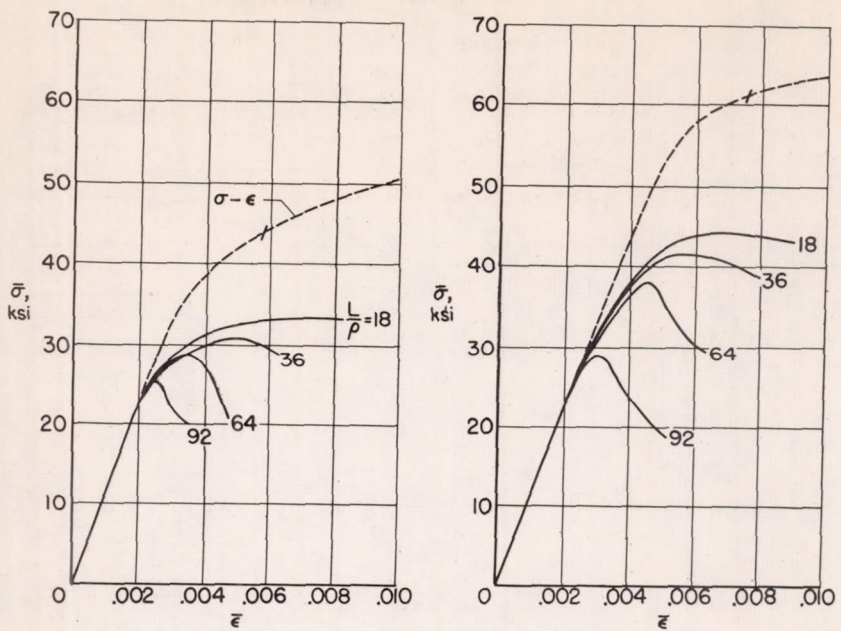
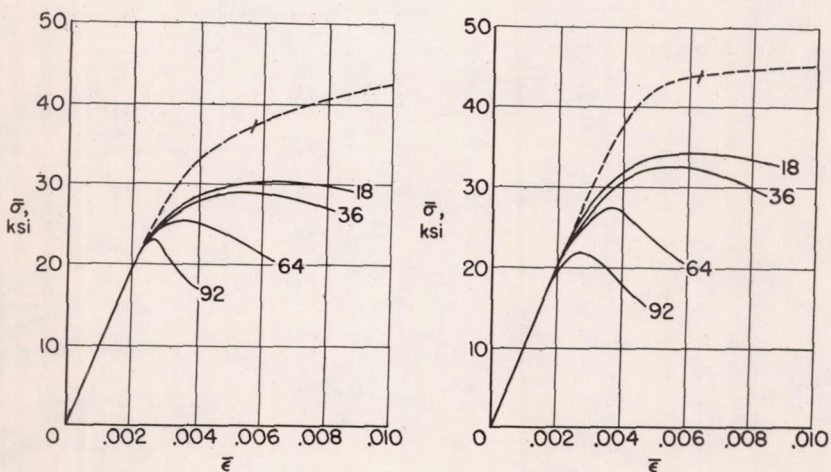


Figure 3.- Test setup. L-78964



(a) Room-temperature tests; exposure at 400° F, none.

(b) Room-temperature tests; exposure at 400° F, 10 hours.



(c) 400° F tests; exposure at 400° F, $\frac{1}{2}$ hour.

(d) 400° F tests; exposure at 400° F, 10 hours.

Figure 4.- Average stress against unit shortening results from compressive strength tests of 2024-T aluminum-alloy panels.

Test temp., °F	Exposure time at 400° F, hr	Symbol		
		Test data	Predicted	
			Eq.(2), $L/\rho = 18$	Eq.(3), $L/\rho > 18$
Room	None	○	○	—
400	$\frac{1}{2}$	□	□	- - -
Room	10	◊	◊	— - -
400	10	△	△	- - -

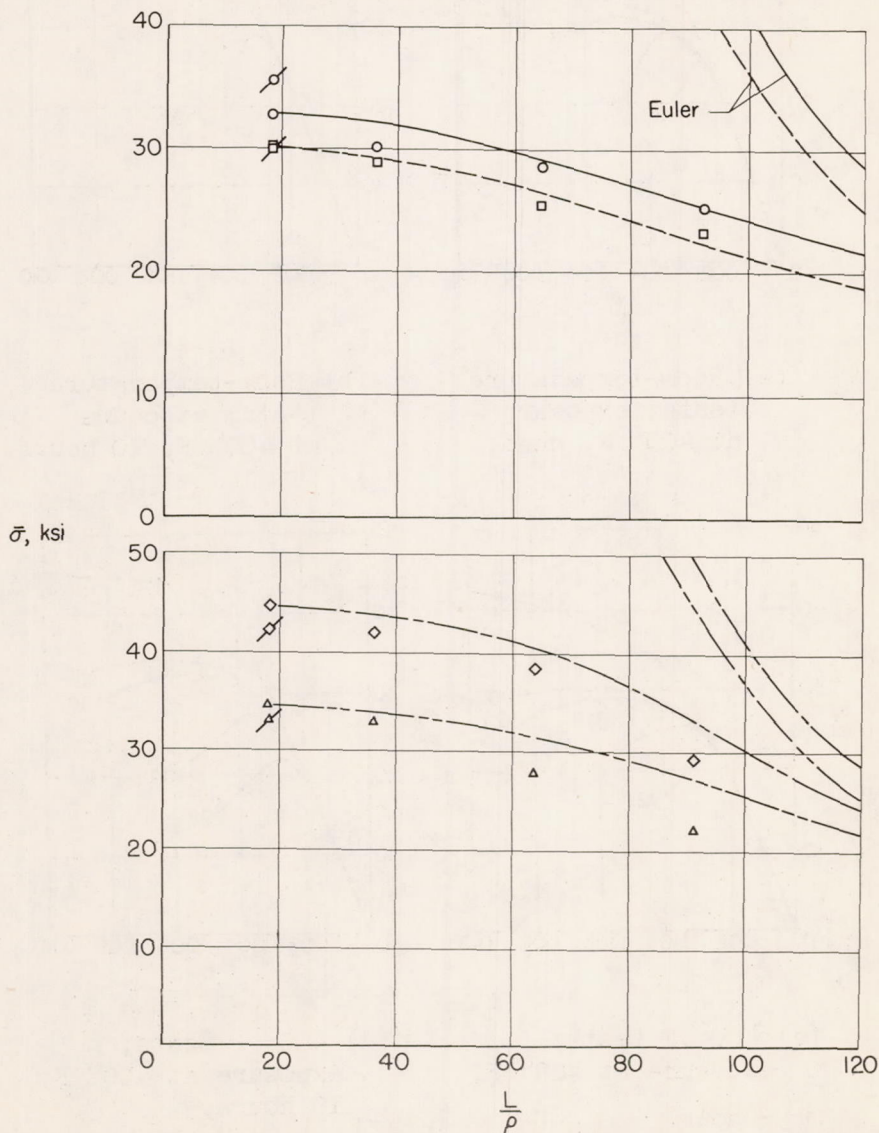
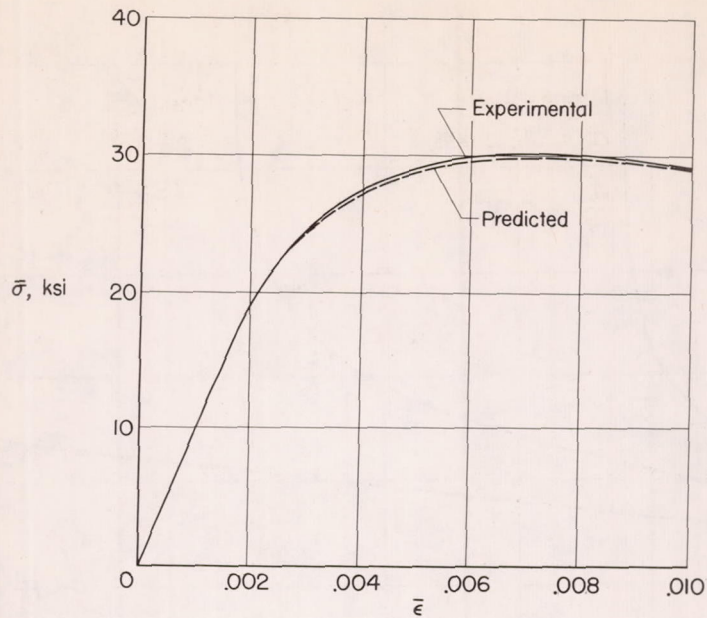
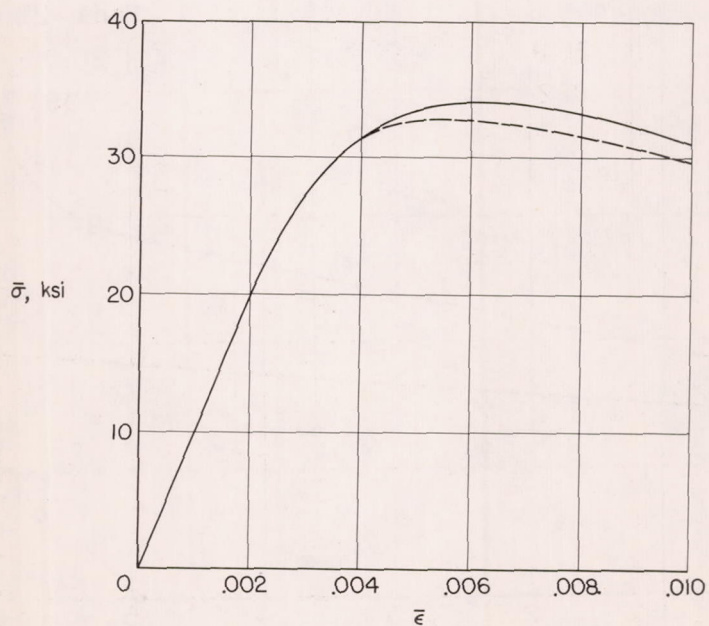


Figure 5.- Comparison of experimental and predicted panel strengths.



(a) 400° F; exposure at 400° F, $\frac{1}{2}$ hour.



(b) 400° F; exposure at 400° F, 10 hours.

Figure 6.- Comparison of experimental and predicted average stress against unit shortening curves. $\frac{L}{\rho} = 18$.

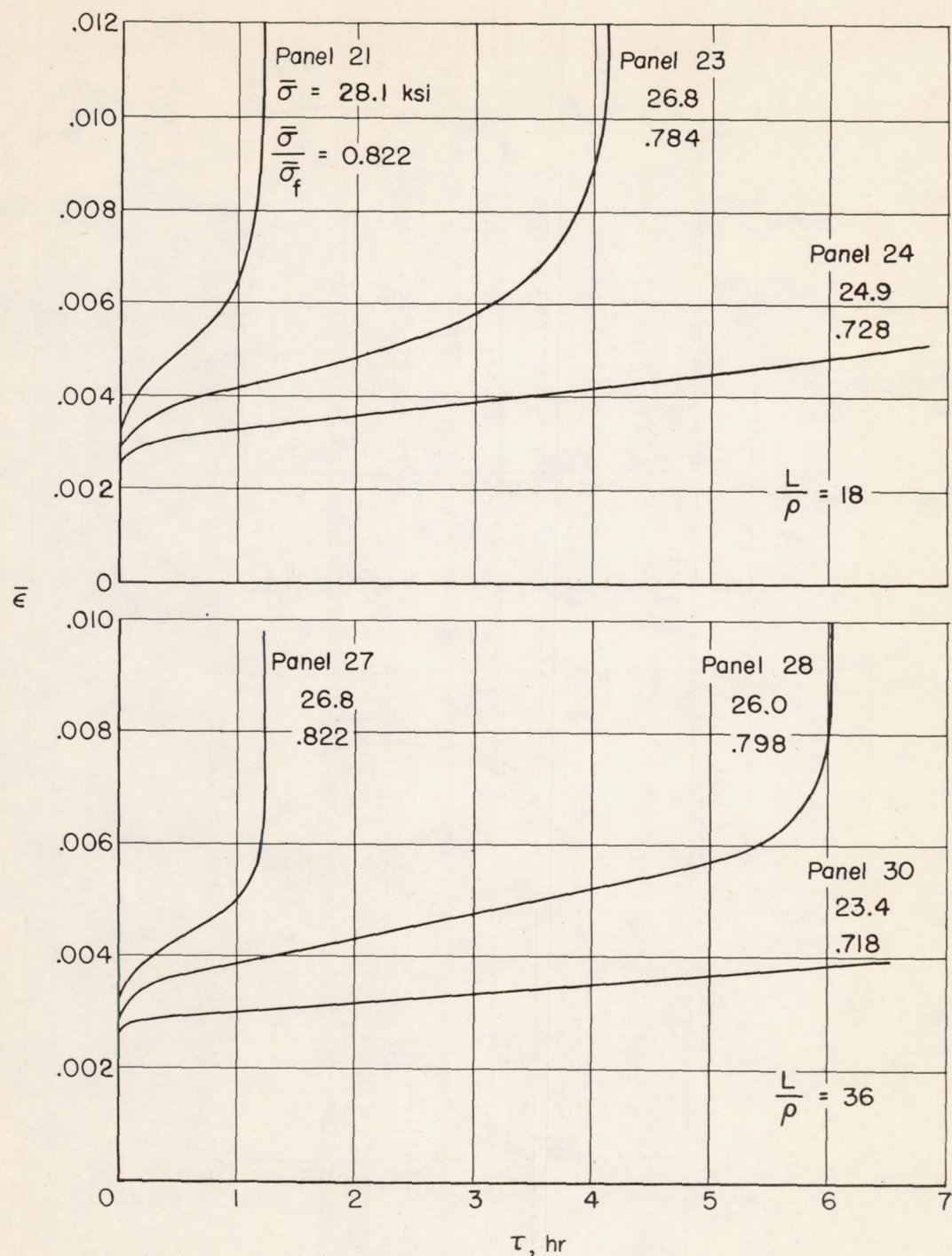


Figure 7.- Typical unit shortening curves from creep tests of panels.
 $T = 400^{\circ}$ F.

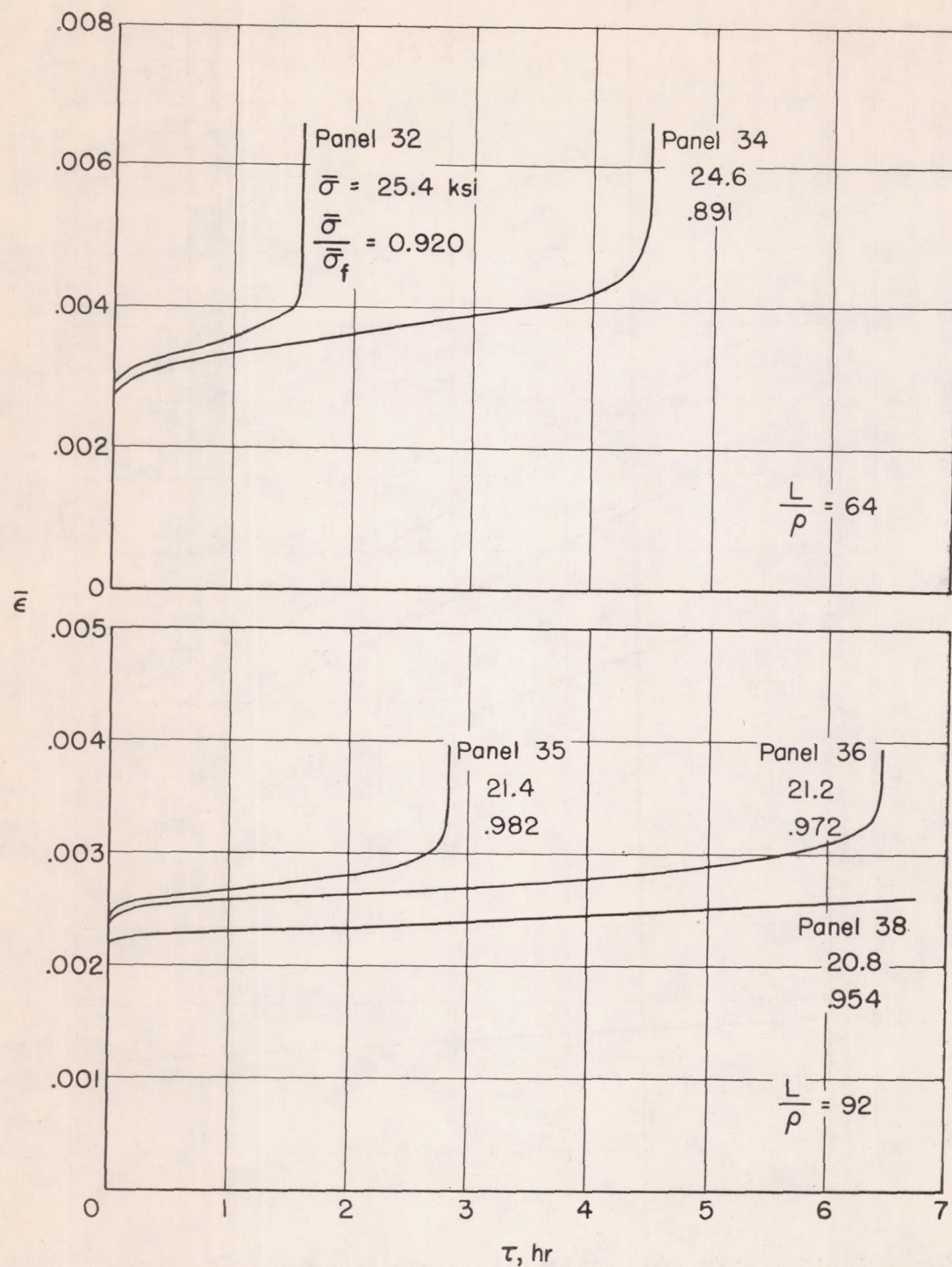


Figure 7.- Concluded.

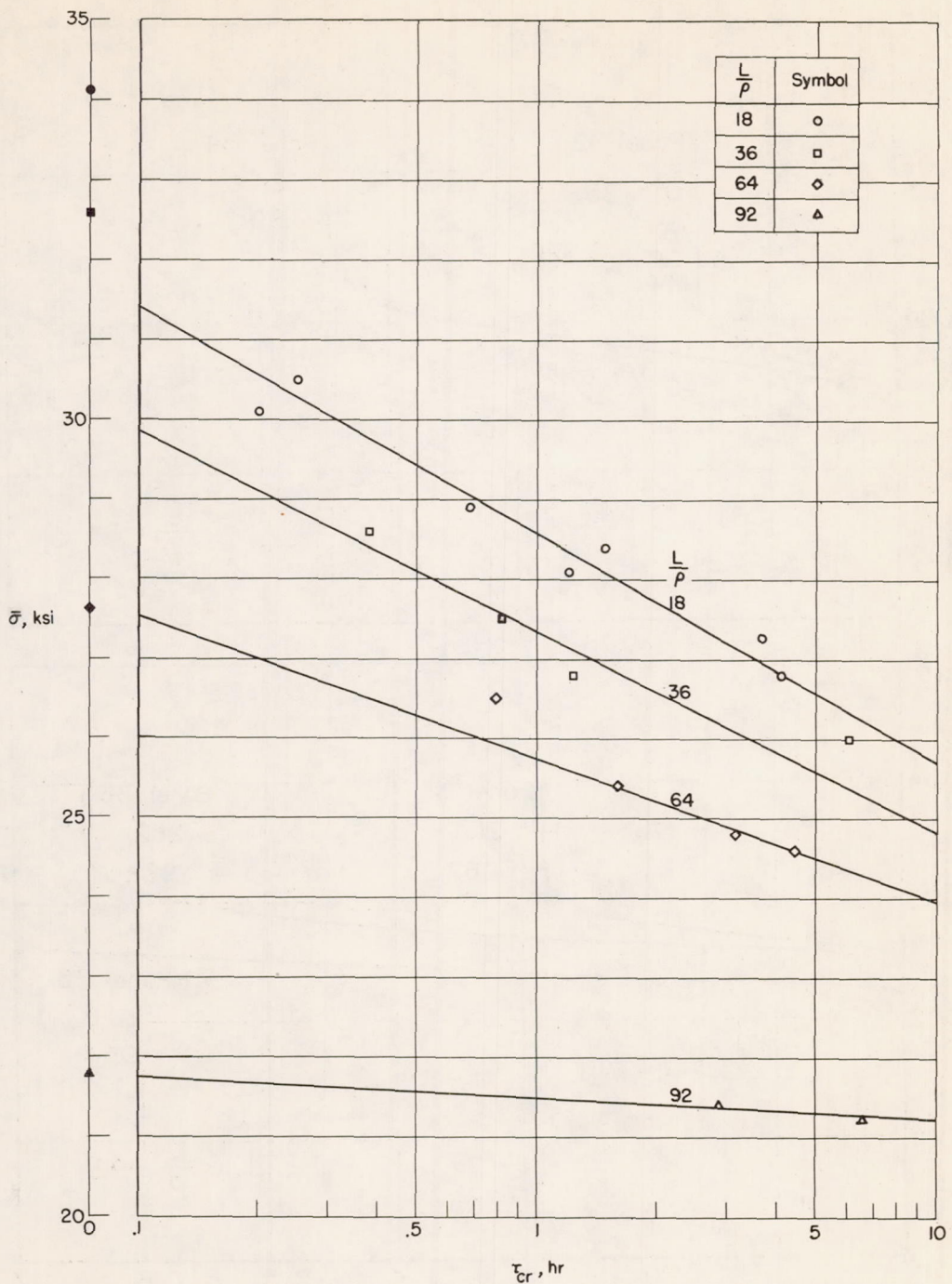


Figure 8.- Lifetime curves for stiffened panels. $T = 400^{\circ}$ F. (The solid symbols on the vertical axis indicate the maximum stress obtained in the compressive strength tests for each slenderness ratio at 400° F.)

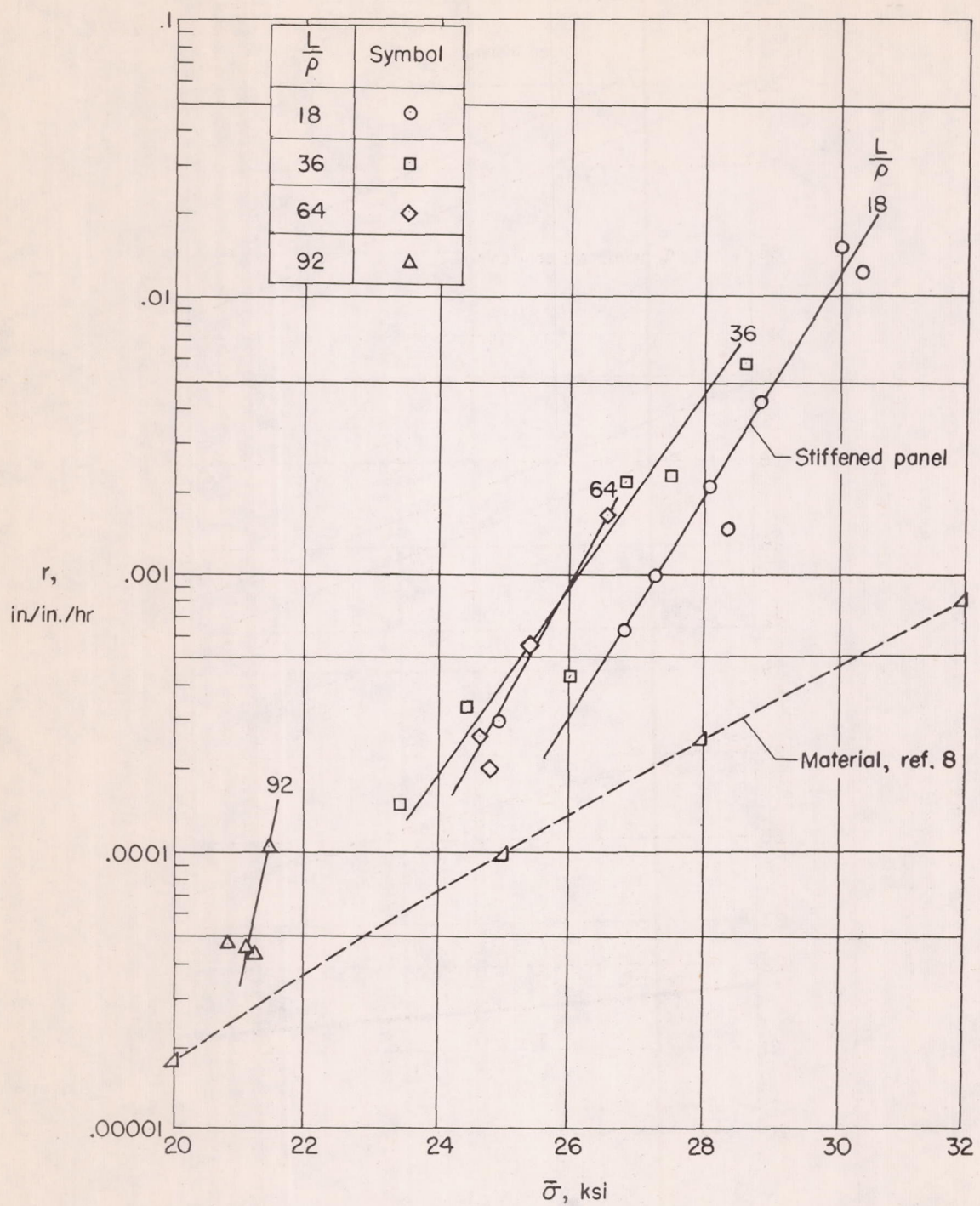


Figure 9.- Minimum creep rates for 2024-T aluminum-alloy panels in compression and 2024-T3 aluminum-alloy sheet in tension. $T = 400^{\circ}$ F.

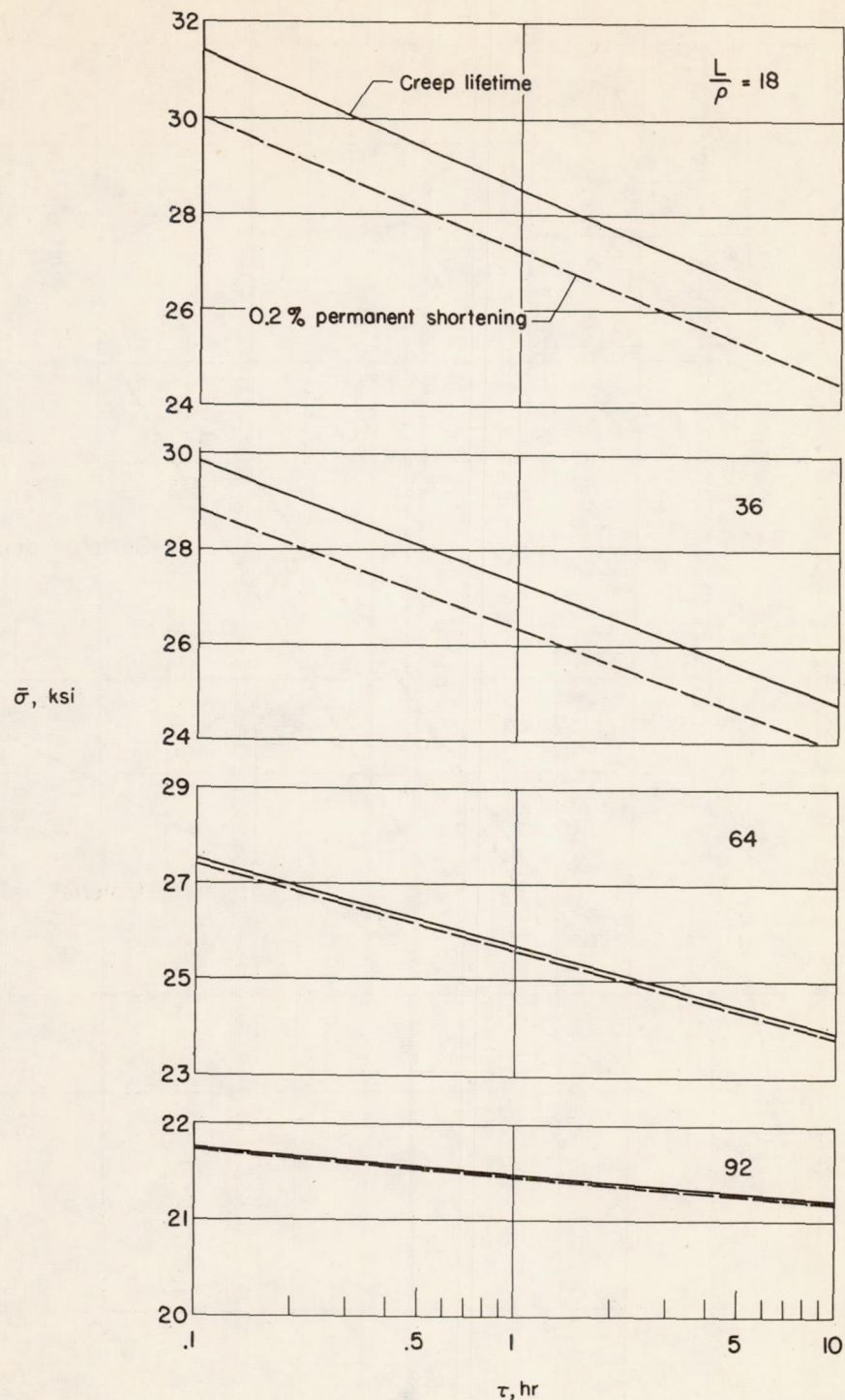


Figure 10.- Comparison of stresses that produce creep failure and 0.2-percent permanent shortening in stiffened panels. $T = 400^{\circ}$ F.

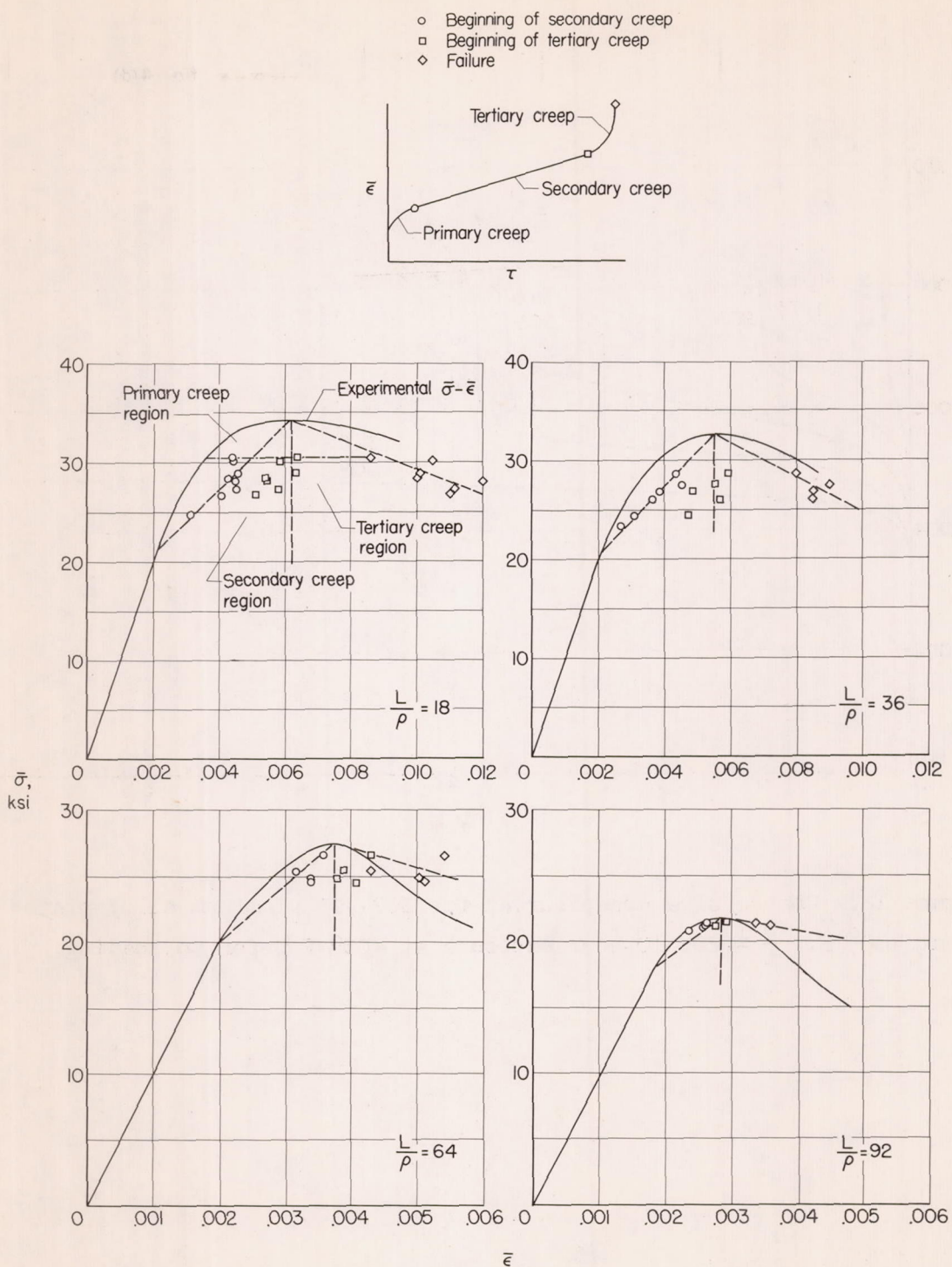


Figure 11.- Unit shortening of stiffened panels at different creep stages.

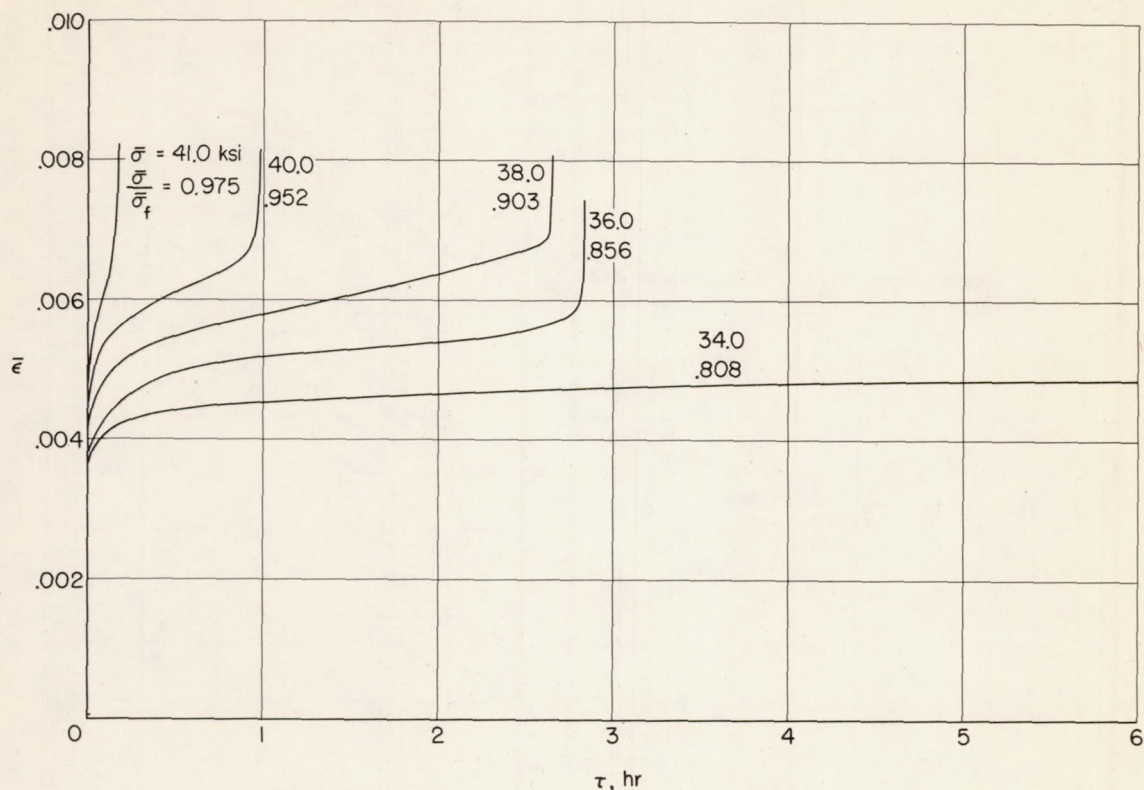


Figure 12.- Compressive creep curves for 2024-T3 aluminum-alloy plates at 400° F. $\frac{b}{t} = 20$; 10-hour exposure at 400° F prior to loading.

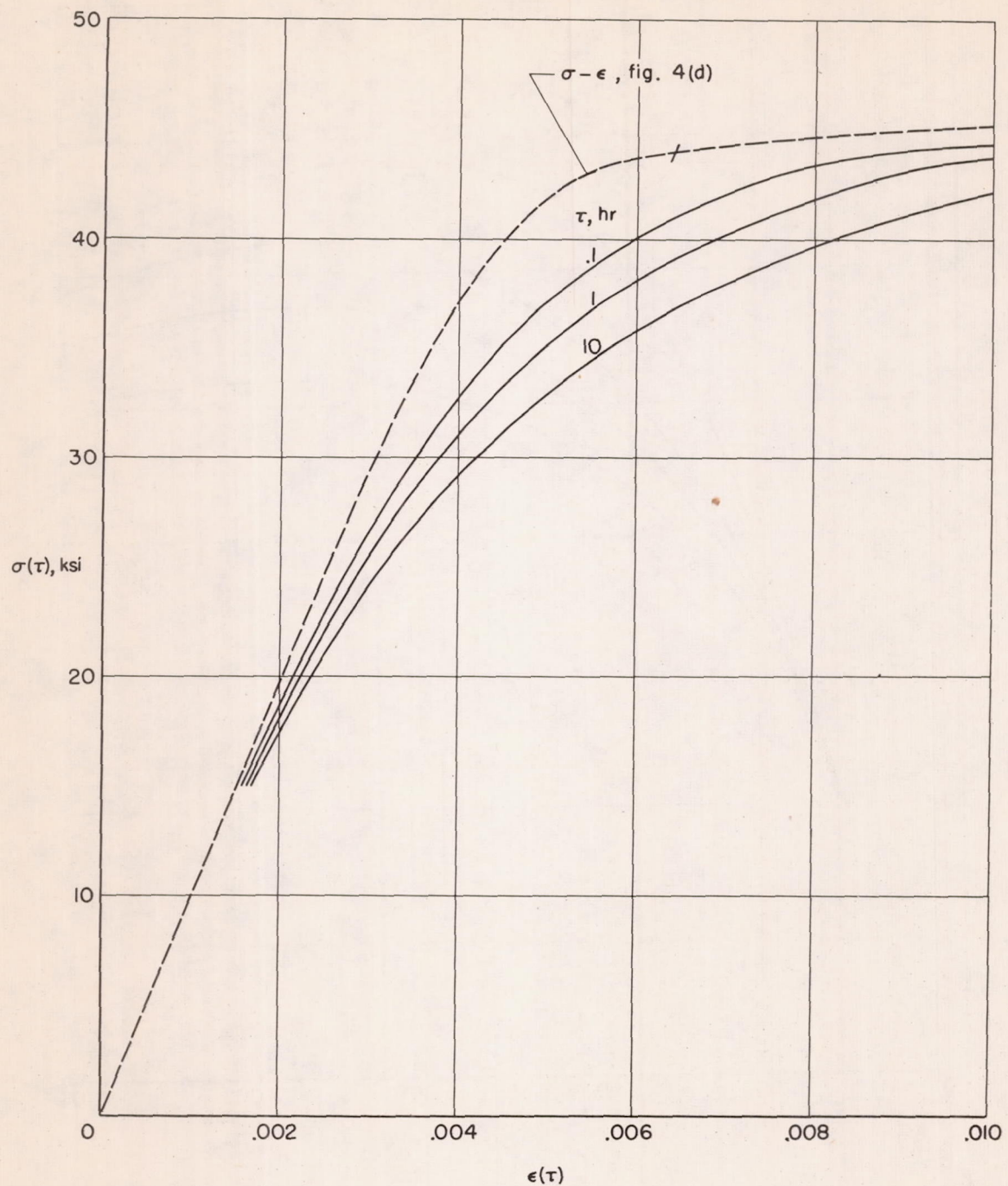


Figure 13.- Time-dependent stress-strain (isochronous) curves for 2024-T3 aluminum alloy at 400° F.

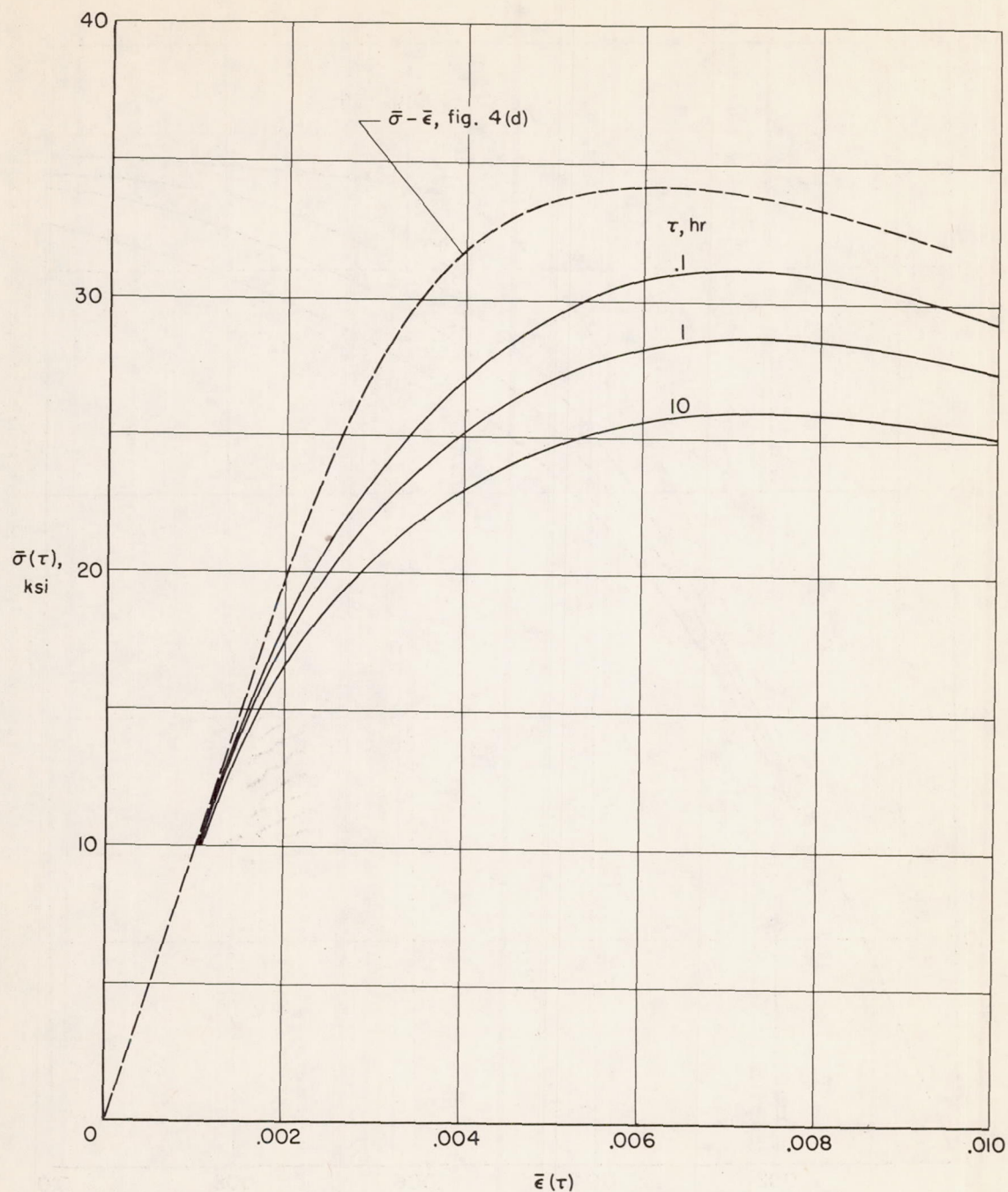


Figure 14.- Curves of time-dependent average stress against unit shortening for stiffened panels at 400° F. $\frac{L}{\rho} = 18.$

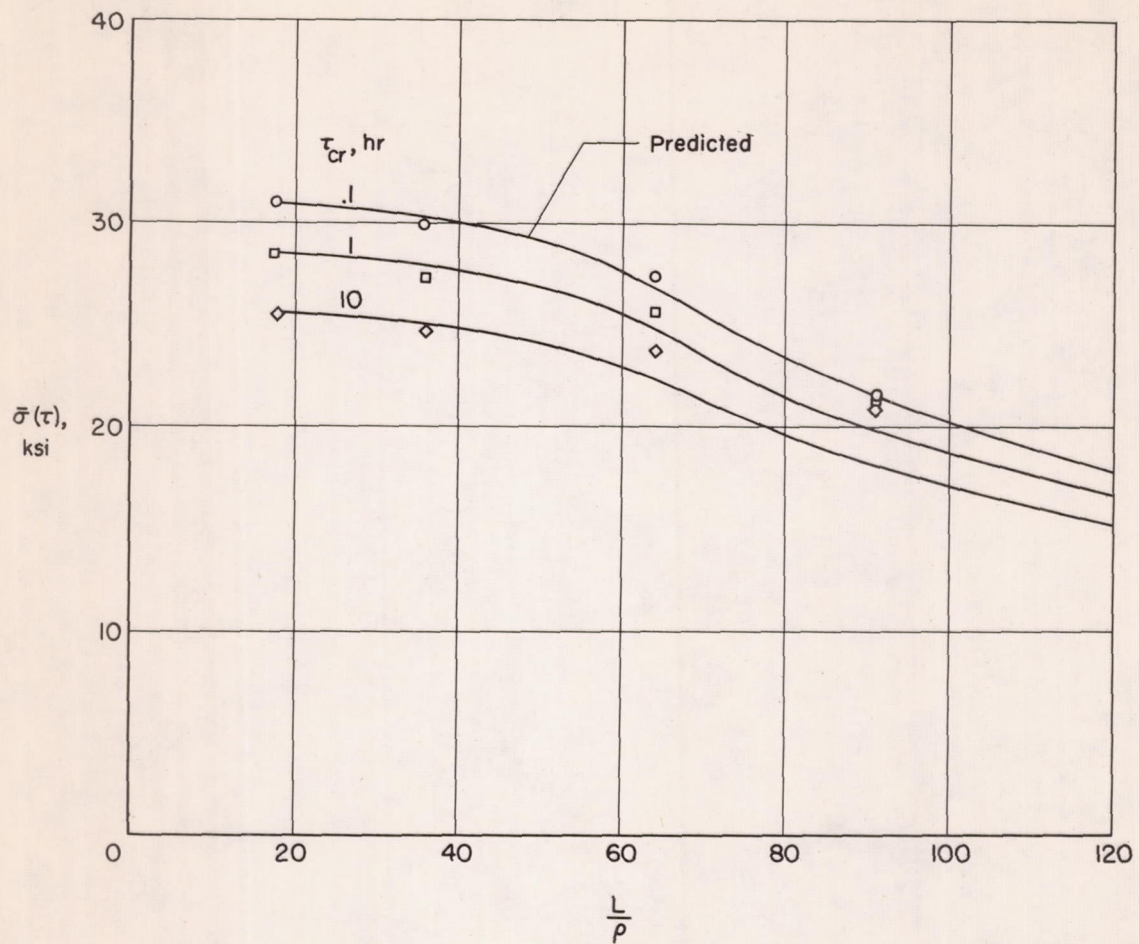


Figure 15.- Comparison of experimental and predicted panel lifetimes.
(The symbols indicate data obtained from the curves given in fig. 8.)

